

Study of microwave transitions in intracavity absorbers with the use of off-resonant response of infrared lasers

E. Arimondo* and Takeshi Oka†

*Herzberg Institute of Astrophysics, National Research Council of Canada,
Ottawa, Ontario K1A 0R6, Canada*

(Received 4 March 1982)

An absorption cell containing low-pressure gas is placed inside a CO₂-N₂O infrared laser cavity and microwave resonances in the gas are detected through the off-resonant response of the infrared laser. The small variation in molecular population in certain rotational levels produced by a microwave pumping changes the bulk susceptibility of the gas through dispersion and thus changes the effective cavity length and the output power of the laser. This new mode of "double resonance" does not require exact coincidence between the laser lines and molecular transitions and is more widely applicable than the normal double-resonance method although its sensitivity is not as great. Characteristics of this method are theoretically studied and compared with experimental results obtained by using the simple molecules CH₃F, D₂CO, D₂O, and NH₃. Microwave resonances are observed through laser lines which are off from molecular infrared transitions by several cm⁻¹. Some unexpected asymmetry of the signals with respect to laser settings has been observed and discussed.

I. INTRODUCTION

The extremely high sensitivity of infrared-microwave [or radio frequency (rf)] double-resonance experiments inside a laser cavity has been well demonstrated and applied to many molecules (see Refs. 1–3 for the earliest work, and Refs. 4–6 for summaries of later work). An absorption cell containing a low-pressure sample gas is placed inside a laser cavity and subjected to microwave radiation (with frequency ν_m). At a microwave resonance, a sharp variation of the laser power is observed because of a variation of molecular population induced by the microwave pumping. This method of observing microwave or rf transitions is at least several orders of magnitude more sensitive than the direct absorption method because (1) the laser "pumps" molecules and produces an anomalous population difference which is larger than that at the thermal equilibrium by a factor of $\sim kT/2h\nu_m$, (2) the three-level system of molecules converts the effect of a microwave photon into that of an infrared laser photon (with frequency ν_l) on the one-to-one basis and thus a gain in energy of ν_l/ν_m is obtained, and (3) the nonlinearity and high- Q response of the laser system further amplifies the signal by a factor of up to $\sim 10^4$ if right conditions are chosen.⁷ While the reasons (1) and (2) above are common to all optical-microwave double resonance, (3) is special for the in-cavity double resonance.

The purpose of the present paper is to consider the case in which the laser radiation is off-resonance from a molecular absorption. This study is motivated from the accidental observation of microwave resonance signals in NH₃ with fair intensity for such a case.¹ If this observation can be generalized, the in-cavity observation of microwave transition is no longer limited to cases of accidental coincidences between laser lines and molecular transition and is applicable with more generality.

Because of the relation

$$\chi \propto [(\Omega_l - \Omega_a) + i\Gamma]^{-1}$$

between the molecular susceptibility χ , the frequency mismatch $\Omega_l - \Omega_a$ between the angular frequencies Ω_l and Ω_a of the laser radiation, and the molecular absorption, respectively, and the damping constant Γ , the effect of dispersion [the real part of χ which falls off as $(\Omega_l - \Omega_a)^{-1}$ for $\Omega_l - \Omega_a \gg \Gamma$] is much larger than that of absorption [the imaginary part of χ which falls off as $(\Omega_l - \Omega_a)^{-2}$] at off resonance. The laser "feels" the presence of the in-cavity gas through dispersion. Thus, among the three reasons for the high sensitivity given earlier (1) does not apply for this case, but (3) applies and (2) applies partially. The variation of molecular population due to the microwave pumping changes the dielectric constant of the bulk gas slightly and thus affect the laser power by varying the effective cavity length of the laser. We examine the strength

and line shape of the signals as functions of the laser tuning, the molecular infrared absorptions and other parameters of the incavity gas. We could observe "double-resonance" signals even when laser lines are off from molecular transition by several cm^{-1} . The double-resonance due to refractive index has also been studied in the microwave region by Macke⁸ who also discussed the case of infrared-microwave double resonance of Ref. 1.

Our experimental results are also relevant for the study of laser operation with an intracavity absorber. The frequency pulling effect produced by the intracavity gas has already been observed in the earliest experiments, for instance by Barger and Hall⁹ on the $3.39\text{-}\mu\text{m}$ He-Ne line with a methane cell. These phenomena have been considered theoretically by Letokhov¹⁰ and Greenstein,¹¹ but the analysis of the experimental results was not clearcut because both absorption and dispersion has to be considered. The analysis of our case is much simpler because the molecular absorption is sufficiently far from the laser line that only the effect of dispersion has to be considered (except for the anomalies discussed in Sec. IV). We leave the intermediate case for future studies, the case in which the interplay of the effects of absorption and dispersion produces peculiar line shapes and shifts of the resonance maximum as observed in the double-resonance experiment of SiH_4 .¹²

In Sec. II of this paper, we describe a theoretical treatment for the laser operation with intracavity absorber and its application to off-resonant double resonance. The experimental apparatus used in this work has been given elsewhere^{1,6} and will not be presented. The experimental results for different molecular systems are presented in Sec. III and analyzed. Special attention will be made to an unexplained phenomenon in Sec. IV.

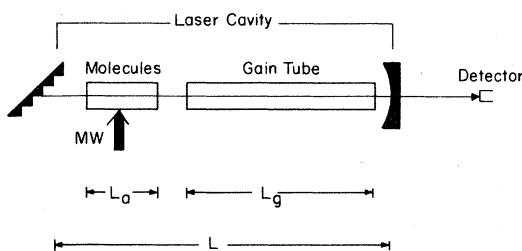


FIG. 1. Double-resonance apparatus. An absorption cell containing low-pressure gas is placed inside the laser cavity. Microwave radiation is applied to the gas and the laser output power is monitored.

II. THEORY

A. Laser operation

Our experiment is schematically shown in Fig. 1. The laser cavity of length L contains a gain cell of length L_g and an absorption cell of length L_a . The effect of the absorption medium on the laser operation is very small because we consider only off-resonant cases. Therefore we study the laser operation using the traditional Lamb's method^{13,14} and treat the effect of the absorption medium as a perturbation.

If the laser oscillation occurs in a single cavity mode with an electric field E , a frequency Ω_l , and a phase ϕ , Lamb's self-consistent equation written as¹⁴

$$\begin{aligned} \dot{E} + \frac{1}{2} \frac{\Omega_l}{Q} E &= -\frac{\Omega_l E}{2} \text{Im}(\chi), \\ \Omega_l + \dot{\phi} &= \Omega_c - \frac{\omega}{2} \text{Re}(\chi), \end{aligned} \quad (1)$$

where Q and Ω_c are the quality factor and the resonance frequency of the laser cavity and χ is the electric susceptibility of media in the laser cavity. In our experimental set up, χ is composed of two parts

$$\chi = \frac{L_g}{L} \chi_g + \frac{L_a}{L} \chi_a, \quad (2)$$

where χ_g and χ_a are the susceptibilities of the gain medium and the absorption, respectively, and L_g/L and L_a/L are their filling factors. We use the solution of Eq. (1) for χ_g given in Ref. 14 and treat χ_a as a perturbation.

The expression for the susceptibility of χ_g is determined from the third-order solution of the density-matrix equations and its subsequent integration over the Maxwellian velocity profile. The first-order term (gain) and the third-order term (saturation) are given in Eqs. (10.28) and (10.38), respectively, in Ref. 14 as rather complicated functions of the laser frequency. Substituting these expressions in Eq. (1) and equating $\dot{E} = 0$, we obtain the steady-state solution of the dimensionless intensity as

$$\begin{aligned} I(\Omega) &= \frac{\mu_g^2 E^2}{2\hbar^2 \Gamma_g^2} \\ &= 4 \frac{1 - \mathcal{N}^{-1} \exp[(\Omega_l - \Omega_0)^2 / (Ku)^2]}{1 + \Gamma_g^2 / [(\Omega_l - \Omega_0)^2 + \Gamma_g^2]}, \end{aligned} \quad (3)$$

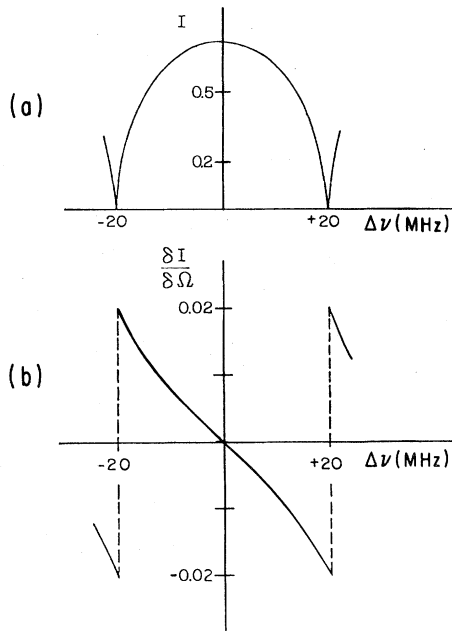


FIG. 2. (a) Laser intensity I as a function of cavity tuning $\Delta\nu = \Omega$ calculated by Eq. (3). Doppler width $Ku/2\pi$ of 30 MHz, the homogeneous width $\Gamma_g/2\pi$ of 15 MHz and the relative excitation parameter of $\eta = 1.12$ have been used; (b) the derivative $\partial I/\partial\Omega$ as a function of $\Delta\nu$. Dispersive double-resonance signal is proportional to this quantity as shown in Eq. (6).

where μ_g , Ω_0 , and Γ_g are the dipole moment, the center frequency, and the damping constant of the gain transition, respectively, Ku is the most probable Doppler shift, and $\mathcal{N} = N_g/N_T$ is the relative excitation, that is, the ratio of the population difference in the gain medium and the threshold population difference for the laser operation. The values of $I(\Omega)$ are plotted in Fig. 2(a) as a function of the laser frequency Ω for a typical condition of our CO_2 laser; $Ku/2\pi = 30$ MHz, $\Gamma_g/2\pi = 15$ MHz, and $N = 1.56$ so that the laser oscillates over the full 40-MHz tuning range of the cavity.

The susceptibility of the off-resonant absorber at the laser frequency Ω is

$$\chi_a(\Omega_l) = \frac{\mu_a^2 N_a}{\epsilon_0 \hbar} \frac{1}{\Omega_a - \Omega_l + i\Gamma_a} \sim \frac{\mu_a^2 N_a}{\epsilon_0 \hbar (\Omega_a - \Omega_l)}, \quad (4)$$

where μ_a and Ω_a are the dipole moment and the center frequency of the absorption transition and N_a is the number density of absorbing molecules. If more than one transitions are close to the laser fre-

quency we should take a sum of terms. Since the imaginary part of χ_a is negligible, we see from Eqs. (1) that the absorber does not affect the laser power directly but only indirectly through a change $\Delta\Omega$ in frequency which is

$$\Delta\Omega = -\frac{\Omega_l}{2(1+S)} \frac{L_a}{L} \chi_a(\Omega_l) = -\frac{\mu_a^2 N_a}{2\epsilon_0 \hbar (1+S)} \frac{L_a}{L} \frac{\Omega_l}{\Omega_a - \Omega_l}, \quad (5)$$

where S is the stabilization factor.¹⁴ The power variation then is

$$\Delta I(\Omega_l) = \frac{\partial I(\Omega_l)}{\partial \Omega_l} \Delta\Omega. \quad (6)$$

The values of $\partial I(\Omega)/\partial\Omega$ are plotted in Fig. 2b. Thus we see that $\Delta I(\Omega_l) = 0$ for the central frequency $\Omega_l = \Omega_0$ and a decrease or increase in laser power is observed depending on which side of the gain curve the cavity is tuned. For a typical value of $\mu_a = 0.2$ debye, $N_a = 3 \times 10^{12} \text{ cm}^{-3}$, $L_g/L \sim \frac{1}{3}$, and $|\Omega_a - \Omega_l| = 0.5 \text{ cm}^{-1}$, we have a calculated frequency shift of $\Delta\nu \sim 40$ kHz. The power variation of the laser could be on the order of 5% on the far sides of the gain curve.

B. Double resonance

The frequency shift $\delta\Omega$ and the resulting power variation ΔI of laser due to microwave pumping are obtained by substituting the resulting change of population δN_a into Eqs. (5) and (6) instead of the total population N_a . The Karplus-Schwinger theory of saturation^{15,16} gives

$$\delta N_a = \mp N_a \frac{\hbar \omega_0}{2kT} \frac{(\mu_m E_m / \hbar)^2}{(\omega_m - \omega_0)^2 + \gamma_a^2 + (\mu_m E_m / \hbar)^2}, \quad (7)$$

where ω_m and E_m are the frequency and the electric field of the applied microwave radiation, respectively, and ω_0 , μ_m , and γ_a are the center frequency, the dipole moment, and the damping constant of the microwave transition, respectively. The \mp sign shows possible decrease or increase of relevant population due to the microwave pumping as shown in Figs. 3(a) and 3(b), respectively. For a sufficiently high microwave power,

$$\mu_m E_m / \hbar \gg \gamma_a$$

and

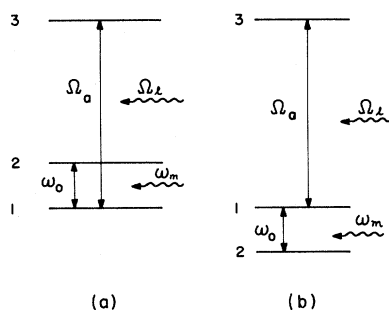


FIG. 3. Energy-level schemes for the infrared-microwave double-resonance experiments with the off-resonant detection. Ω_l and ω_m are applied infrared and microwave frequencies, respectively, and Ω_a and ω_0 are the resonant infrared and microwave frequencies, respectively.

$$\delta\Omega = \pm \frac{N_a \omega_0 L_a}{4\epsilon_0 k T L (1+S)} \frac{\Omega}{\Omega_a - \Omega} \sum_M \frac{|\langle R_3 M | \mu_a | R_1 M \rangle \langle R_1 M | \mu_m | R_2 M \rangle|^2 E_m^2 / \hbar^2}{(\omega_m - \omega_0)^2 + \gamma_a^2 + |\langle R_1 M | \mu_m | R_2 M \rangle|^2 E_m^2 / \hbar^2}, \quad (9)$$

where $\Delta M = 0$ transitions are considered both for the infrared transition and the microwave transition because the two radiation electric fields are parallel with each other. R_1 , R_2 , and R_3 are rotational quantum members of the levels 1, 2, and 3, respectively.

III. EXPERIMENTAL RESULTS

A. $^{12}\text{CH}_3\text{F}$

We started the experiment from CH_3F which has the well-known ν_3 band absorption in the 9.6- μm region and has a large infrared transition moment and a large permanent dipole moment. The rotational transition $(J, K) = 1, 0 \leftarrow 0, 0$ in the ground vibrational state was pumped by an OKI 50-V 10 klystron at 51.072 GHz.¹⁶ Double-resonance signals have been observed on several CO_2 laser lines whose positions relative to the CH_3F absorption are accurately known from the laser Stark spectroscopy.¹⁷ Figure 4 shows the strong signal observed on the output of the laser oscillating on the 9 $P(16)$ CO_2 line, which is 4.4 GHz off the ${}^qR(0,0)$ $\nu_3 \leftarrow 0$ infrared transition. The microwave radiation was frequency modulated and swept, and the resulting change in laser power was processed by a phase sensitive detector and displayed on an oscilloscope. In accordance with the discussion given in the previous section, no double-resonance signal was detected when the laser cavity was tuned at the center of the CO_2 gain curve [Fig. 4(b)] and signals

$$\delta N_a \sim \mp N_a \hbar \omega_0 / 2kT$$

for the resonance $\omega = \omega_0$. Thus the frequency shift of the laser is given by

$$\begin{aligned} \delta\Omega &= \frac{\hbar \omega_0}{2kT} \Delta\Omega \\ &= - \frac{\mu_a^2 N_a}{2\epsilon_0 \hbar (1+S)} \frac{\hbar \omega_0}{2kT} \frac{L_a}{L} \frac{\Omega}{\Omega_a - \Omega}. \end{aligned} \quad (8)$$

For the experimental condition given in the previous subsection, the frequency shift is on the order of 100 Hz and the power variation $10^{-4} \sim 10^{-5}$ which is easily detectable.

When $\mu_n E_m / k \gg \gamma_a$ does not apply, the microwave pumping is not perfect; we then use Eq. (7) and obtain more general formula

with approximately equal amplitude and opposite phase were observed when the laser was set on the two sides of the gain curve as shown in Figs. 4(a) and 4(c). The apparent asymmetry in the derivative line shape of the signal was due to a nonlinear sweep caused by a capacitive coupling of the sawtooth sweep voltage and is not genuine.

The effect of microwave pumping was observed also in several other CO_2 laser lines in the 9.6 μm region. Figure 5 shows intensities of the observed signals. From the behavior of the signals upon laser tuning we could determine the sign of the frequency shift. We tried to operate the laser in the same condition for all different lines so that apart from a common scaling factor, the measurements shown in Fig. 5 represent the frequency shift produced by the microwave pumping. The solid curves in Fig. 5 show the calculated values using Eq. (8). In this calculation, we had to take into account three infrared transitions ${}^qR(0,0)$, ${}^qR(1,0)$, and ${}^qP(1,0)$ which are all connected to the rotational transition in the ground state. Note that ${}^qR(0,0)$ corresponds to the case of Fig. 3(a) whereas the other two to Fig. 3(b) so that they have opposite effect on $\delta\Omega$. Note also that only molecules with $M = 0$ contribute to the signal because the $R(0)$ rotational transition was pumped and the infrared and microwave fields were parallel.

In order to measure the absolute value of the shift in the laser frequency caused by the microwave pumping we have compared the signal with that

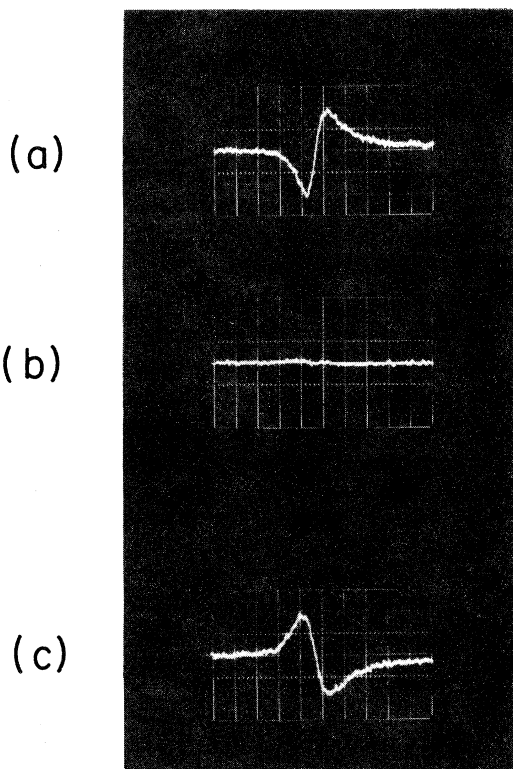


FIG. 4. Signals of $^{12}\text{CH}_3\text{F}$. Sample pressure 35-mTorr, laser line $P(16)$ line at 1050.44 cm^{-1} , $\nu_l - \nu_0 = 4.4\text{ GHz}$ from the ν_3 $R(0,0)$ transition, microwave transition $J, K = 1, 0 \leftarrow 0, 0$ at 51.072-GHz, time constant 10 m sec, sweep time 5 MHz/cm. No signal was observed when the laser was set at the center of the cavity mode, (b) and signals with equal amplitude and opposite phase were observed when the laser was set on the two sides of the cavity mode.

produced by applying a modulation voltage on the piezoelectric mount of the output mirror. The latter signal can be converted to the frequency shift from the measured voltage of modulation and the known response characteristics of the piezoelectric material. From this analysis we obtained a shift of $160 \pm 35\text{ Hz}$ caused by microwave pumping of a gas of 25-mTorr pressure detected on the $P(16)$ CO_2 laser line. On the other hand, using the transition dipole moment of 0.144 debye calculated from the intensity measurement of Hodges and Tucker¹⁸ we obtain from Eq. (8) a predicted value of 114 Hz which is in agreement with our observation.

One anomaly was observed in higher pressure region. We observed that in such a region the double-resonance signal does not have the same intensity when the laser is tuned to the two opposite sides of the cavity gain curve. Figure 6 shows this

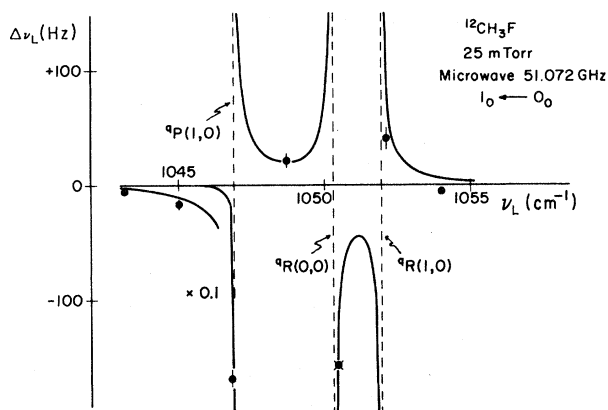


FIG. 5. Intensities and signs of double-resonance signals observed on CO_2 laser lines (points from the left) $P(24)$, $P(22)$, $P(20)$, $P(18)$, $P(16)$, $P(14)$, and $P(12)$. Vertical bars show the uncertainties in the measurements. Solid lines are the theoretical calculation using Eq. (9). Theoretical curves have been scaled to the observed values for the $P(16)$ line. Vertical scale for the frequency shift (in Hz) of laser radiation was obtained from the absolute measurement on the $P(16)$ line as discussed in the text. Uncertainty in the absolute vertical scale is 20%.

behavior for the $P(16)$ CO_2 laser line. The asymmetry parameter η plotted in Fig. 6 is defined as

$$\eta = \frac{I_h - I_l}{I_h + I_l}, \quad (10)$$

where I_h and I_l are signal intensities on the high-frequency side and on the low-frequency side of the gain curve, respectively. As noted in Fig. 6, at high pressure, the signal on the high-frequency side is approximately three times stronger than that at the low-frequency side. This behavior will be discussed in Sec. IV in detail.

The pressure dependence of the absolute signal intensity is as expected. The signal increases linearly with pressure at the low pressure region due to the increased density of absorber, reaches a maximum, and then decreases and the microwave saturation becomes incomplete as expected from Eq. (7).

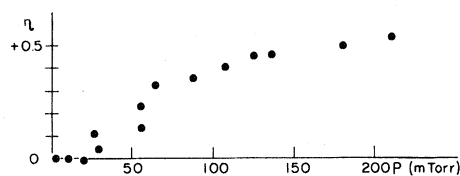


FIG. 6. Observed asymmetry in intensities of the observed signals when the laser was on the high- or low-frequency side of the cavity mode. Results for the $P(16)$ CO_2 laser line at 1050.44 cm^{-1} .

B. $^{13}\text{CH}_3\text{F}$

Signals observed for $^{13}\text{CH}_3\text{F}$ were similar to those for $^{12}\text{CH}_3\text{F}$ given above. One interesting case, however, was the collision-induced double-resonance signal observed on the 9 $P(32)$ CO_2 laser line. This laser line is coincident with the $^9R(4,3)$ transition in the ν_3 band of $^{13}\text{CH}_3\text{F}$ (Ref. 19) within the Doppler profile and thus the double-resonance signal is caused through absorption rather than dispersion. The discussion of such a signal is outside the scope of this paper, but this weak signal is useful for comparing the effects of dispersion and absorption.

A signal was observed on the $P(32)$ CO_2 laser line when the microwave radiation pumped the $J, K=1, 0 \leftarrow 0, 0$ transition of $^{13}\text{CH}_3\text{F}$ at 49.725 GHz.¹⁶ The fact that this signal was not caused by dispersive response of the laser was obvious from the behavior of the signal on the cavity tuning. The signal did not change sign on the two sides of the gain curve and simply decreased the intensity when the laser frequency was shifted away from the center of the $^9R(4,3)$ line. This signal must be caused by the collision-induced transfer of the nonthermal molecular population in the $(J, K)=(1, 0)$ and $(0, 0)$ levels by the microwave pumping to the $(J, K)=(4, 3)$ level. It is known that such transfer always has some preference rule²⁰ and leads to a nonthermal population in other levels. In this case the collision-induced signal was weak because $\Delta k=3$ and $\Delta J > 1$ collision-induced transitions are involved. When compared with the dispersive signal observed on the $P(38)$ laser line [which is 9 GHz off from the $^9R(0, 0)$ transition], the collision-induced signal observed for a mixture of 10 mTorr of $^{13}\text{CH}_3\text{F}$ and 30 mTorr of He was about five times weaker. Note that for the collision-induced double resonance, the laser operates near the Q -switching region and is very sensitive.⁷

C. D_2CO

The band origin of the ν_4 out-of-plane vibrational mode of D_2CO is at 938 cm^{-1} ,²¹ and this band can be studied with $10.4\text{-}\mu\text{m}$ CO_2 or N_2O laser line. We pumped the $1_{01} \leftarrow 0_{00}$ transition at 58 468.68 MHz (Ref. 22) by an OK1 55V10 klystron and detected the effect on the laser output power of several CO_2 and N_2O laser lines. Here we found that most of the signals were caused by collision-induced double-resonance effect rather than by off-resonance dispersive effect. The distinction between these effects were clear from the behavior of the signal as a function of laser tuning. The results are

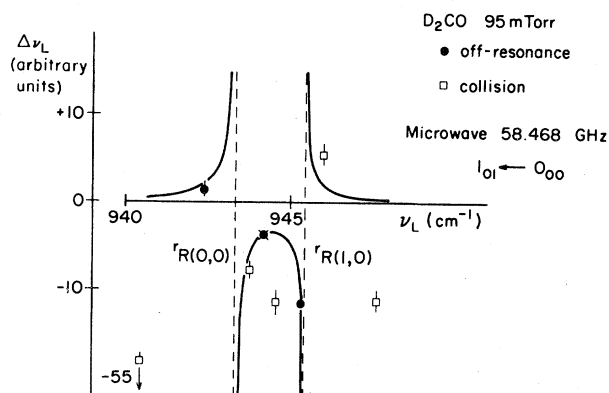


FIG. 7. Intensities and signs of double-resonance signals observed for D_2CO on (points from the left) CO_2 $P(24)$, $P(22)$, N_2O $R(5)$, CO_2 $P(20)$, N_2O $R(6)$, $R(7)$, CO_2 $P(18)$, and $P(16)$ lines. Black circles represent off-resonant dispersive signals and open squares represent collision-induced signals. Former signals are plotted for increase or decrease of the laser frequency and the latter that of intensity. Solid curves represent the theoretical calculation which was scaled to the value observed for the $P(20)$ line. Sample pressure 95 mTorr, microwave power 200 mW, microwave transition $1_{01} \leftarrow 0_{00}$ at 58 468.68 MHz.

summarized in Fig. 7 where the dispersive signals are shown with black circles and the collision-induced signals are shown with squares.

The dispersive signals can be explained as due to the $^9R(0, 0)$ and $^9R(1, 0)$ transition. The theoretical curves are shown with solid curves. The dispersive signals are considerably weaker than those for CH_3F because of the weakness of the ν_4 band of D_2CO . From the relative intensities of the infrared spectra of H_2CO and CH_3F listed by Pugh and Rao,²³ we estimate the ν_4 band of D_2CO to be 20 times weaker than the ν_3 band of CH_3F . This explains the measured intensities of the dispersive signals.

Collision-induced signals were found on $P(16)$, $P(18)$, and $P(24)$ CO_2 laser lines and $R(5)$, $R(6)$, and $R(7)$ N_2O laser lines. Unlike the case of CH_3F they are stronger than dispersive signals partly due to the weakness of the latter discussed above but presumably also partly due to more efficient transfer of non-Boltzmannian population from the pumped levels to the other levels. For the $P(18)$ CO_2 laser line the collision produces an increase in the laser power thus indicating a decrease in the molecular population in lower level while for the other lines they are opposite. Whether this was due to the parity preference rule²⁰ or due to the heating of the

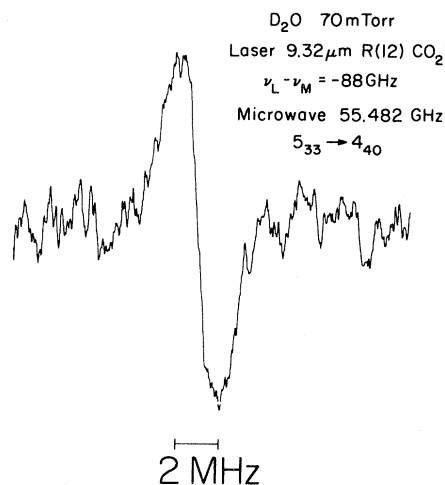


FIG. 8. Microwave transition $4_{40} \leftarrow 5_{33}$ at 55.842 GHz of D_2O observed on the $R(12)$ CO_2 laser line at 1073.28 cm^{-1} . This laser line is 2.95 cm^{-1} off the ν_2 $3_{31} \leftarrow 4_{40}$ infrared transition of D_2O . Sample pressure 70 mTorr, time constant of detection 1 sec.

gas²⁴ was not clear. An attempt was made at assigning these coincidences by using the analysis of Coffey *et al.*²¹ and Nakagawa²⁵ but was not possible. The coincidence between the $P(16)$ CO_2 line and the D_2CO gas has subsequently been assigned by Orr and Nutt²⁶ to be the ν_4 $^7Q(12,2)$ transition.

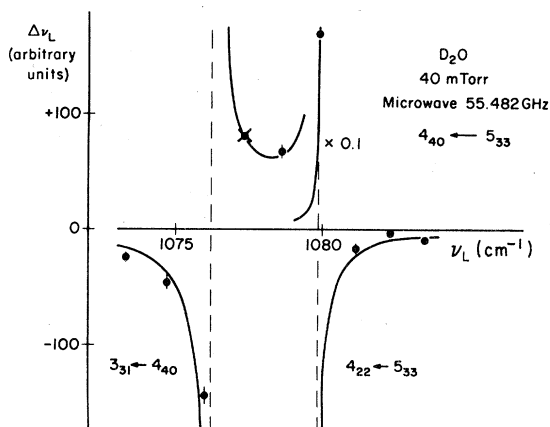


FIG. 9. Intensities and signs of double-resonance signals observed for D_2O on (points from the left) CO_2 $R(12)$, $R(14)$, $R(16)$, $R(18)$, $R(20)$, $R(22)$, $R(24)$, $R(26)$, and $R(28)$ lines. Solid curves represent the theoretical calculation which was scaled to the value observed for the $R(18)$ laser line. Absolute value of the shift in the laser frequency was not precisely measured but was approximately 100 Hz comparable to the CH_3F signals.

D. D_2O

D_2O has the strong ν_2 band extending over the $9 \mu\text{m}$ region. The $R(22)$ CO_2 laser line at 1079.85 cm^{-1} is only 320 MHz off the ν_2 $4_{22} \leftarrow 5_{33}$ transition as measured by Keilmann *et al.*²⁷ by the acousto-optic modulation of the laser radiation. The $4_{40} \leftarrow 5_{33}$ rotational transition has a resonance frequency of 55482.32 MHz .²⁸ This transition has a small matrix element because of $\Delta K_c = 3$ but with sufficient microwave power and low-sample pressure, we could see not only a very strong off-resonance signal on the $R(26)$ line but also signals on other laser lines which are much further away. Figure 8 shows an example where the laser line was 2.95 cm^{-1} off the interacting D_2O transition. From the analysis of the ν_2 band of D_2O by Lin and Shaw²⁹ we found that the ν_2 $3_{31} \leftarrow 4_{40}$ transition also contributes to the off-resonant signal. Figure 9 shows the relative intensities of the off-resonant signals observed on several CO_2 laser lines in the $9.6\text{-}\mu\text{m}$ region. Since the microwave saturation was not complete because of the small matrix element, we used Eq. (9) for the calculation. The theoretical curves explain the observed results satisfactorily.

E. NH_3

The off-resonant signals of NH_3 have been reported earlier.¹ Here we limit the discussion only to microwave resonances with $J=5$ and different K values. The relative positions of the NH_3 infrared absorption lines and laser lines are accurately known from the infrared-microwave two-photon spectroscopy.^{1,30} Other molecular constants have been accurately determined from laser spectroscopy³¹ and the recent comprehensive study using a submillimeter spectrometer, and infrared grating spectrometer, and a diode laser spectrometer.³² We observed strong signals due to the large transition dipole moment of 0.239 debye³³ and the smaller rotational partition function. Thus, for example, the off-resonance signal observed on the $P(32)$ CO_2 laser line for the microwave inversion transition for $J=5$ and $K=3$ with 20 mTorr of NH_3 sample was 150 times stronger than the CH_3F signal discussed earlier and given in Fig. 4. The NH_3 signal corresponded to the laser frequency shift of 25 kHz that could be measured directly on a stable laser.

While the observed intensities agree with the calculated using Eq. (9), we observed an unexpected behavior of the signals as a function of laser tuning. This anomaly is similar to that for CH_3F discussed

earlier in Sec. III A in that it is related to the asymmetry between the signals on the high frequency and low-frequency side of the gain curve, but it is different in that it is line shape rather than intensity which is different. Also the off-resonant signal was observed even when the laser was tuned to the center of the cavity.

A typical example is shown in Fig. 10. For the upper trace [Fig. 10(a)], the laser was tuned to the low-frequency side of the cavity mode and the usual derivative line shape was observed. When the laser was tuned to the high-frequency side, the observed signal had the same intensity and opposite phase but the resonance curve was narrower as a function of the microwave frequency. When the laser was tuned to the center of gain curve, we saw the signal given in Fig. 2(b) which had the appearance of mixed first- and second-derivative shapes. This shape can be analyzed as due to the overlap of the "broad" and "narrow" signals that were observed on the two sides of the gain curve.

We see this behavior on all studied laser lines and inversion transitions whenever the inversion transition was saturated strongly by the microwave radiation corresponding NH_3 pressure of 1 mTorr to several tens mTorr. The saturation broadening of the broad and narrow resonances had the same dependence on the microwave power and the ratio of the linewidth of the broad resonance to that of the narrow resonance was constant and equal to ~ 2.5 . A slight misalignment in the optical cavity of the laser changed the relative intensities of the two signals but did not change the overall behavior. The second derivative line shape reported earlier by

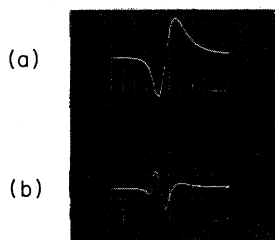


FIG. 10. Anomalous signal in NH_3 observed on the CO_2 $R(30)$ line at 1084.63 cm^{-1} when the (5,3) inversion transition was pumped. Sample pressure 10 mTorr, $\nu_1 - \nu_0 = 1.3 \text{ GHz}$ from the ν_2 sa $^9R(5,3)$ transition, time constant 10 m sec, sweep time 0.5 sec. Signal (a) is the normal signal observed for the laser oscillating on the low-frequency side of the cavity mode. Signal (b) is the anomalous signal which was observed when the laser was set at the center of cavity mode. Scale in (b) is magnified by a factor of 2.

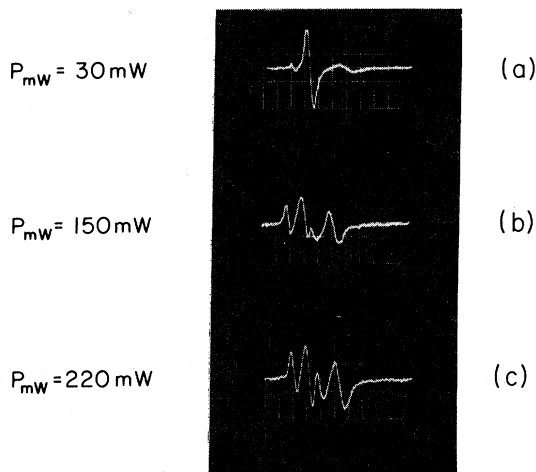


FIG. 11. Hyperfine structure of NH_3 (5,1) inversion transition observed on the output power of the $R(30)$ CO_2 laser line at 1084.63 cm^{-1} . Sample pressure 13 mTorr, $\nu_1 - \nu_0 = 0.5 \text{ GHz}$ from the ν_2 sa $^9R(5,1)$ transition, microwave frequency 19.838 GHz. Note that as the microwave pump power is increased from (a) to (c) the strongest central component changes its shape, while the weaker $\Delta F = \pm 1$ satellites simply increase their intensities.

Freund and Oka¹ is the result of the overlap of the broad and narrow signals.

The fact that this peculiar shape results from the saturation of the microwave transition was seen clearly when we studied the nuclear hyperfine structure of the microwave resonance. The case of microwave resonance for the $J=5$, $K=1$ inversion transition is shown in Fig. 11. This microwave transition is composed of the strong central line for overlapping $\Delta F=0$ transition and two weak satellites corresponding to the $\Delta F=\pm 1$ transitions. When the microwave pump power was increased from Fig. 11(a) to 11(c), the weaker satellites simply increase their intensities while the stronger central component changes its shape to second derivative.

IV. DISCUSSION ON THE OBSERVED ASYMMETRY

The observed asymmetry of the signals with respect to the laser tuning for CH_3F and NH_3 are qualitatively different. For CH_3F the asymmetry appears at higher pressure and in intensities of the signals, whereas for NH_3 the asymmetry appears at lower pressure and in the widths of the signals. We discuss in this section possible effects which cause these anomalies.

The asymmetry in intensities of the two signals of CH_3F which appears at high pressure must be caused by the addition of absorption effect to the dispersive effect. For the double-resonance signal discussed in Sec. III A and shown in Fig. 4, the laser line is 4.4 GHz above the ${}^9R(0,0)$ transition. Although this is off resonant, the Lorentzian tail of the absorption is still sizable at the laser frequency for higher pressure. Since the microwave pumping of the $J=1\leftarrow 0$ transition decreases the population of the $J=0, K=0$ level the dissipative load of the laser decreases and laser power is increased regardless of whether the laser is tuned to the higher-frequency side or lower-frequency side of the gain curve. The dispersive effect, on the other hand, increases the laser power on the high-frequency side [because $\partial I/\partial\Omega$ shown in Fig. 2(b) is negative and $\Delta\nu_l$ shown in Fig. 5 is negative] and decreases the laser power on the low-frequency side. The magnitude of the absorption effect adds to that of the dispersive effect on the high-frequency side and subtracts on the low-frequency side and this leads to the asymmetry.

The off-resonant absorption coefficient γ can be estimated from

$$\gamma = \frac{4\pi^2\omega}{3hc} N_a |\mu_{ij}|^2 \frac{2\Gamma_g}{(\Omega_l - \Omega_0)^2 + \Gamma_g^2}. \quad (11)$$

Using the pressure broadening parameter of 20 Mhz/Torr (Ref. 34) we calculate $\Gamma_g/2\pi$ for the pressure of 0.2 Torr and the absorption at the laser frequency (4.4 GHz off the center) to be $\Gamma_g^2/(\Omega_l - \Omega_0)^2 \sim 8.3 \times 10^{-7}$ of the resonant absorption coefficient. From the vibrational transition moment of 0.144 debye the off-resonant absorption coefficient is calculated to be $\gamma = 9 \times 10^{-8} \text{ cm}^{-1}$. Thus, the variation of the absorption coefficient due to the microwave pumping is of the order of $\gamma h\nu/2kT \sim 4 \times 10^{-10} \text{ cm}^{-1}$. Considering the path length of 1 m and the cavity quality factor of ~ 20 this corresponds to an absorption of $\sim 8 \times 10^{-7}$. The resonance characteristics⁷ and nonlinearity of laser operation will further amplify this number to produce a significant change in the output power of the order of $10^{-4} \sim 10^5$.

The asymmetry observed in NH_3 which appears at low pressure in the linewidth is more difficult to interpret. Since the width of microwave pumping efficiency should be the same regardless of the laser setting, some very nonlinear effect must be operating in order to produce the large observed ratio in widths of 2.5 reported in Sec. III E. The only such strongly nonlinear effect we could think of was the

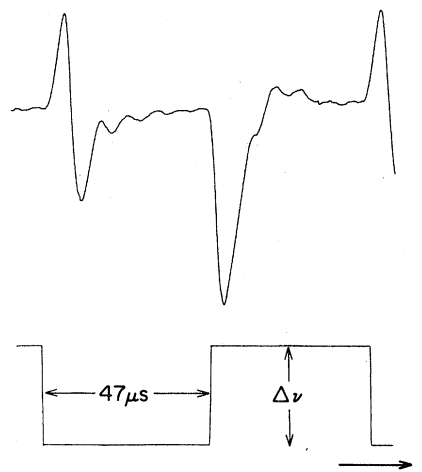


FIG. 12. Transient response observed on the output power of the CO_2 $R(16)$ line at 966.25 cm^{-1} when the microwave radiation pumping the $(5,4)$ inversion transition at $22\,653.00 \text{ MHz}$ was modulated on-off at 10.5 kHz . The laser line is 600 MHz off the ν_2 ${}^9Q(5,4)$ transition. Note the difference in the transient behavior when the laser frequency was pushed to or pulled from the cavity center.

transient response of the laser to the modulation introduced by the microwave pumping. The importance of such an effect in double resonance has already been demonstrated.⁷

In order to clarify this point, we studied the transient response of the $R(9)$ CO_2 laser line to the pumping of the NH_3 $(5,4)$ inversion transition. Figure 12 shows a typical result in which the microwave pumping was switched on and off at the rate of 10.6 kHz and thus shifted the laser frequency towards or away from the center of the gain curve. It was noticed that the transient responses for the two steps were very different. This difference was consistently observed when the microwave frequency was scanned over the resonance line and when the laser frequency was tuned inside the gain curve. Since the lock-in detection of the double-resonance signal detects the transient signal, this asymmetry must contribute to the asymmetry of the signals when the laser is tuned on the opposite sides of the cavity mode. Our observation that the dependence of the signal intensity on the laser tuning was different as we varied the modulation frequency from $10 \sim 60 \text{ kHz}$ also seems to support this idea. However, we have not been able to explain the observed asymmetry in more details. The line-shape distortion produced in saturated absorption by the transit time through a curved wave front of radiation³⁵ seems to be irrelevant to our problem.

The influence of the asymmetry observed in intracavity Lamb dip and the dependence of saturation on the Gaussian distribution of the light and on the diffraction effects³⁶ may have to be considered carefully.

V. CONCLUSION

We have shown that microwave transitions in intracavity absorber can be detected using the off-resonant response of infrared lasers. The small variation of molecular population produced by a microwave pumping changes the bulk susceptibility of the gas through dispersion and thus changes the effective cavity length and the laser output power. This method was tested for the observations of the $J, K = 1, 0 \leftarrow 0, 0$ transition of CH_3F and $^{13}\text{CH}_3\text{F}$, the $1_{01} \leftarrow 0_{00}$ transition of D_2CO , the $4_{40} \leftarrow 5_{33}$ transition of D_2O and the $J, K = 5, K$ inversion transitions of NH_3 . The observed behavior of the signals were explained by a theory in which the effect of laser gain medium treated to the third order of density matrix and the effect of absorber as a perturbation. Unexpected asymmetry has been observed for CH_3F at high pressure and for NH_3 at low pressure between the signals observed when the laser was set at the high-frequency side of the gain curve and that at the low-frequency side. The intensity asymmetry for CH_3F was explained as due to the overlap of the effect of absorption and that of dispersion and the linewidth asymmetry for NH_3 was ascribed to the

asymmetry of laser transients caused by the microwave switching.

As a method of double resonance, the off-resonant detection has the following advantages:

(1) We do not have to rely on the rare accidental coincidence between the laser lines and the molecular absorption and thus the method is more generally applicable.

(2) We do not need the accurate frequency of the infrared transition to see the double resonance. Thus, in an intracavity double-resonance experiment using a tunable laser³⁷ the two-dimensional search for resonance can be made easier.

(3) The coupling of the microwave and the infrared radiation through a three-level system of absorber is much weaker and theoretical analysis is simpler. This allows a highly accurate frequency measurement.

The disadvantages are as follows.

(1) Since the laser does not produce population anomaly, the sensitivity is much smaller than that of the normal double resonance.

(2) For the same reason, this method is applicable only to microwave and millimeter wave region where $h\nu/kT$ is sizable and cannot be used effectively in the radio-frequency region.

ACKNOWLEDGMENT

We wish to thank G. W. Hills for pointing out to us that the D_2O molecule is useful for our study.

*Present address: Istituto di Fisica Sperimentale, Università di Napoli, Italy.

†Present address: Department of Chemistry and Department of Astronomy and Astrophysics, The University of Chicago, Chicago, Illinois 60637.

¹S. M. Freund and T. Oka, *Appl. Phys. Lett.* **21**, 60 (1972); *Phys. Rev. A* **13**, 2178 (1976).

²M. Takami and K. Shimoda, *J. Appl. Phys. Jpn.* **11**, 1648 (1972); **12**, 603 (1973); *J. Mol. Spectrosc.* **59**, 35 (1976); M. Takami, K. Uehara, and K. Shimoda, *J. Appl. Phys. Jpn.* **12**, 924 (1973).

³R. F. Curl, Jr., and T. Oka, *J. Chem. Phys.* **58**, 4908 (1973); R. F. Curl, Jr., T. Oka, and D. S. Smith, *J. Mol. Spectrosc.* **46**, 518 (1973); R. F. Curl, Jr. *ibid.* **48**, 165 (1973).

⁴T. Oka, *Frontiers in Laser Spectroscopy*, Les Houches Summer School Proceedings Session XXVII, edited by R. Balian, S. Haroche, and S. Liberman (North-Holland, Amsterdam, 1977).

⁵H. Jones, *Modern Techniques of Microwave Spectroscopy*,

edited by G. W. Chantry (Academic, New York, 1979).

⁶E. Arimondo, P. Glorieux, and T. Oka, *Phys. Rev.* **17**, 1375 (1978).

⁷E. Arimondo and P. Glorieux, *Appl. Phys. Lett.* **33**, 49 (1978).

⁸B. Macke, *Appl. Phys.* **13**, 271 (1977).

⁹R. L. Barger and J. L. Hall, *Phys. Rev. Lett.* **22**, 4 (1969).

¹⁰V. S. Letokhov, *Zh. Eksp. Teor. Fiz.* **54**, 1244 (1968) [*Soviet Phys. — JETP* **27**, 665 (1968)].

¹¹H. Greenstein, *J. Appl. Phys.* **43**, 1732 (1972).

¹²W. A. Kreiner and T. Oka, *Can. J. Phys.* **53**, 2000 (1975).

¹³W. E. Lamb, Jr., *Phys. Rev.* **134A**, 1429 (1964).

¹⁴M. Sargent III, M. O. Scully, and W. E. Lamb, Jr., *Laser Physics* (Addison-Wesley, Reading, Mass., 1974).

¹⁵R. Karplus and J. Schwinger, *Phys. Rev.* **73**, 1020 (1948).

¹⁶C. H. Townes and A. L. Schawlow, *Microwave Spectroscopy* (McGraw-Hill, New York, 1955).

- ¹⁷S. M. Freund, G. Duxbury, M. Römheld, J. T. Tiedje, and T. Oka, *J. Mol. Spectrosc.* **52**, 38 (1974).
- ¹⁸D. T. Hodges and J. R. Tucker, *Appl. Phys. Lett.* **27**, 667 (1975).
- ¹⁹S. M. Freund, M. Römheld, and T. Oka, *Phys. Rev. Lett.* **35**, 1497 (1975).
- ²⁰T. Oka, *Advan. At. Mol. Phys.* **9**, 127 (1973).
- ²¹D. Coffey, Jr., C. Yamada, and E. Hirota, *J. Mol. Spectrosc.* **64**, 98 (1977).
- ²²K. Takagi and T. Oka, *J. Phys. Soc. Jpn.* **18**, 1174 (1963).
- ²³L. A. Pugh and K. Narahari Rao, *Molecular Spectroscopy; Modern Research*, edited by K. Narahari Rao (Academic, New York, 1976), Vol. II, p. 165.
- ²⁴W. A. Kreiner, A. Eyer, and H. Jones, *J. Mol. Spectrosc.* **52**, 40 (1974).
- ²⁵T. Nakagawa (private communication).
- ²⁶B. J. Orr and G. F. Nutt, *J. Mol. Spectrosc.* **84**, 272 (1980).
- ²⁷F. Keilmann, R. L. Sheffield, J. R. R. Leite, M. S. Feld, and A. Javan, *Appl. Phys. Lett.* **26**, 19 (1975).
- ²⁸G. Erlandson and J. Cox, *J. Chem. Phys.* **25**, 778 (1956).
- ²⁹C. L. Lin and J. H. Shaw, *J. Mol. Spectrosc.* **66**, 441 (1977).
- ³⁰H. Jones, *Appl. Phys.* **15**, 261 (1978).
- ³¹K. Shimoda, Y. Ueda, and J. Iwahori, *Appl. Phys.* **21**, 181 (1980).
- ³²S. Urban, V. Spirko, D. Papousek, R. S. McDowell, N. G. Nereson, B. P. Belov, L. I. Gershstein, A. V. Maslovskij, A. F. Krupnov, J. Curtis, and K. Narahari Rao, *J. Mol. Spectrosc.* **79**, 455 (1980).
- ³³T. Shimizu, F. O. Shimizu, R. Turner, and T. Oka, *J. Chem. Phys.* **55**, 2822 (1971).
- ³⁴O. R. Gilliam, H. D. Edwards, and W. Gordy, *Phys. Rev.* **75**, 1014 (1949).
- ³⁵J. L. Hall and C. J. Bordè, *Appl. Phys. Lett.* **29**, 788 (1976); C. J. Bordè, J. L. Hall, C. V. Kunasz, and D. Hummer, *Phys. Rev. A* **14**, 236 (1976).
- ³⁶A. Le Floch, R. Le Naour, J. M. Lenormand, and J. P. Tachè, *Phys. Rev. Lett.* **45**, 544 (1980).
- ³⁷R. L. DeLeon, P. H. Jones, and J. S. Muentner, *Appl. Opt.* **20**, 525 (1981).

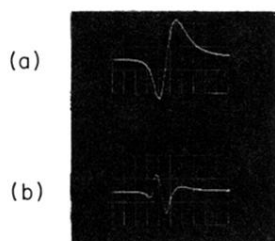


FIG. 10. Anomalous signal in NH_3 observed on the CO_2 $R(30)$ line at 1084.63 cm^{-1} when the $(5,3)$ inversion transition was pumped. Sample pressure 10 mTorr, $\nu_1 - \nu_0 = 1.3 \text{ GHz}$ from the ν_2 sa $^9R(5,3)$ transition, time constant 10 m sec, sweep time 0.5 sec. Signal (a) is the normal signal observed for the laser oscillating on the low-frequency side of the cavity mode. Signal (b) is the anomalous signal which was observed when the laser was set at the center of cavity mode. Scale in (b) is magnified by a factor of 2.

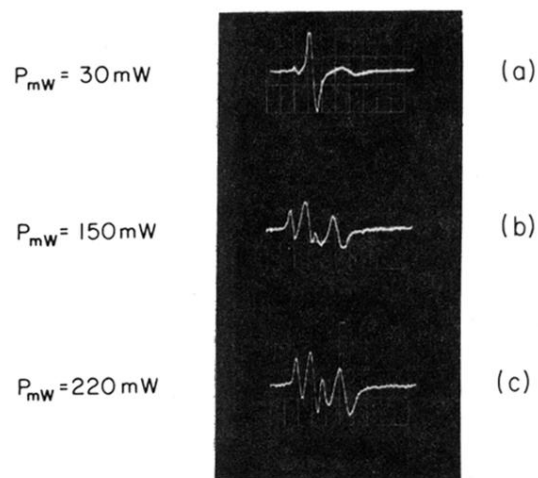


FIG. 11. Hyperfine structure of NH_3 (5,1) inversion transition observed on the output power of the $R(30)$ CO_2 laser line at 1084.63 cm^{-1} . Sample pressure 13 mTorr, $\nu_1 - \nu_0 = 0.5 \text{ GHz}$ from the ν_2 sa ${}^9R(5,1)$ transition, microwave frequency 19.838 GHz. Note that as the microwave pump power is increased from (a) to (c) the strongest central component changes its shape, while the weaker $\Delta F = \pm 1$ satellites simply increase their intensities.

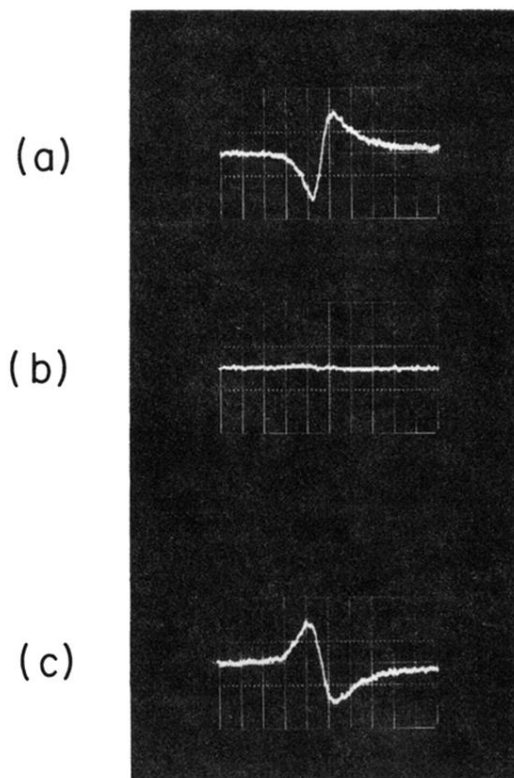


FIG. 4. Signals of $^{12}\text{CH}_3\text{F}$. Sample pressure 35-mTorr, laser line $P(16)$ line at 1050.44 cm^{-1} , $\nu_l - \nu_a = 4.4$ GHz from the ν_3 $'R(0,0)$ transition, microwave transition $J, K = 1, 0 \leftarrow 0, 0$ at 51.072-GHz, time constant 10 m sec, sweep time 5 MHz/cm. No signal was observed when the laser was set at the center of the cavity mode, (b) and signals with equal amplitude and opposite phase were observed when the laser was set on the two sides of the cavity mode.